Summary Report

Applications of High Strength Concrete for Highway Bridges

Harold J. Jobse
Director of Engineering Services
Concrete Technology Corporation
Tacoma, Washington

Saad E. Moustafa
Chairman
Department of Civil Engineering
University of New Orleans
New Orleans, Louisiana

The U.S. Department of Transportation authorized Concrete Technology Corporation to identify through analytical development and laboratory investigation applications of high strength concrete for highway bridges. The applications were to optimize the use of 10,000-psi (70 MPa) concrete for advancement in the development of bridge members.

NOTE: This paper is based on a report prepared for the Offices of Research and Development, Federal Highway Administration, United States Department of Transportation. The full report (Number FHWA 82/096) is available at cost of duplication through the National Technical Information Service, Springfield, Virginia 22161.

Over the years, the practical design compressive strength of portland cement concrete has steadily increased from 3 to 6 ksi (21 to 42 MPa). Now it is feasible to produce and design concrete with compressive strengths of 10 ksi (70 MPa) and higher. Concrete of this strength requires careful selection of high quality mixing materials and more rigid quality control. High strength concrete has been used successfully in the columns of a 76-story office building and in a 461-ft (140 m) liquid petroleum gas storage vessel.

High strength concrete has been made and used by prestressed concrete producers for many years. However, the

producers use the high *early* strength of the concrete so that the formwork may be removed, the concrete members prestressed, and the forms reused every day without taking advantage of the eventual 8 to 10 ksi (56 to 70 MPa) compressive strength in the structural design.

OBJECTIVE

The objective of the project was to demonstrate the advantages of high strength concrete in highway bridges by identifying analytically those members or systems most likely to benefit. Certain analytical predictions would be tested and the results applied in the form of design recommendations and proposed code changes. The investigation was limited to plant precast members since those products showed the most potential for effective use of high strength concrete. Practical techniques for manufacturing and constructing members with high strength concrete were to be included in the report to illustrate the advantages in a way which would lead to immediate use.

Synopsis

This report summarizes the results of a study to determine the potential for high strength concrete in highway bridges. Current data and applications are reviewed and related to AASHTO specifications. Conceptual designs are developed to explore the potential for such possibilities as increased span lengths; wider girder spacings; reduced cross-sectional areas of compression members; and thinner plates for segmental construction, arch bridge members and piers.

The capacity of thin concrete plates in buckling is studied. Comprehensive interaction diagrams developed through a computer program are used to determine the controlling factor for square hollow piers made with thin plates of high strength concrete. The diagrams were confirmed by laboratory load tests under varying eccentricities.

Also presented are code proposals and concepts for the more rapid adaptation of high strength concrete for use in highway bridges.

MIXING AND PLACING HIGH STRENGTH CONCRETE

Guidelines for mixing and placing high strength concrete are based on the following parameters:[1-3]

Constituents: Cement, aggregates, and admixtures that will produce concrete of the required strength and insure consistency of properties over a period of time must be selected. The maximum size of coarse aggregate must be small, usually not greater than 0.5 in. (13 mm). Superplasticizers may be used.

Water-cement ratio: The water-cement ratio must be low, usually between 0.30 and 0.35, by weight.

Cement content: The cement content must be high, usually between 800 and 950 lb per cu yd (475 and 565 kg/m^3).

Consolidation: Good consolidation in sturdy forms is necessary to produce adequately dense concrete.

Quality control: A well-managed quality control program, including planning and cooperation of all parties involved, is essential to success.

PHYSICAL PROPERTIES OF HIGH STRENGTH CONCRETE

The properties of high strength concrete, similar to the properties of normal strength concrete, can be predicted by anyone familiar with concrete engineering. Ratios of tensile strength to

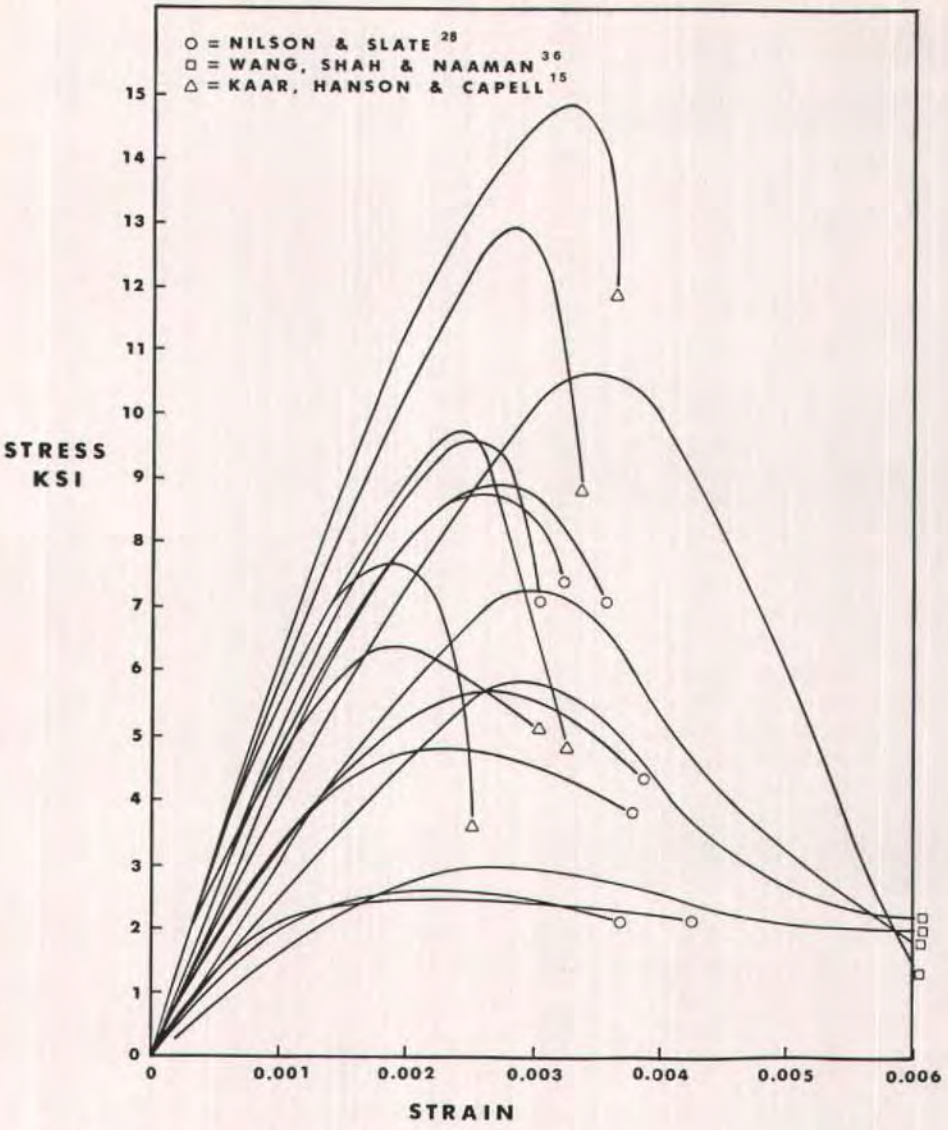

Fig. 1. Stress-strain curves for high strength concrete.

square root compressive strength for high strength concrete are similar to those obtained for normal strength concrete.[4] Stress-strain relationships for high strength concrete are shown in Fig. 1.[4-6] The initial slope of the curves becomes steeper with increasing compressive strength (modulus of elasticity increases), and the strain at maximum stress tends to increase slightly. Also, the slope of the descending portion of the curves is steeper for the high strength concretes than for normal strength concretes, so the high strength concrete in effect is more brittle.

Data indicate that the modulus of elasticity for 10-ksi (70 MPa) concrete is represented better by the formula:[4,6,7]

$$E_c = 26\, w^{1.5} \sqrt{f'_c} \quad \text{(U.S. units)}$$

or

$$E_c = 0.0337\, w^{1.5} \sqrt{f'_c} \quad \text{(S.I. units)}$$

than by the equation:

$$E_c = 33\, w^{1.5} \sqrt{f'_c} \quad \text{(U.S. units)}$$

or

$$E_c = 0.0428\, w^{1.5} \sqrt{f'_c} \quad \text{(S.I. units)}$$

presently suggested by the AASHTO Specifications[8] and the ACI Code[9] for normal strength concrete. High strength concretes creep less than normal strength concretes when loaded to a given percentage of compressive strength.[4] Shrinkage of high strength concrete is about the same as that of normal strength concrete.[4,7]

ADVANTAGES AND DISADVANTAGES OF HIGH STRENGTH CONCRETE

One advantage of high strength concrete is its greater compressive strength, which can be evaluated in relation to unit cost, unit weight, and unit volume. High strength concrete, with its greater compressive strength per unit cost, is the least expensive means of carrying compressive force. In addition, its greater compressive strength per unit weight and unit volume allows lighter, more slender bridge members.

Other advantages of high strength concrete include increased modulus of elasticity and increased tensile strength. Increased stiffness is advantageous when deflections or stability govern the bridge design, and increased tensile strength is advantageous in service load design in prestressed concrete.

A disadvantage of high strength concrete is that the mix has much less water than normal strength concrete. This results in mixes that have reduced workability and handling time, making them more difficult to place and properly compact. In addition, high quality aggregates in necessary sizes and cement that will consistently produce concrete of the required strength may not be available in some localities.

Structural design considerations may preclude effective use of the increased concrete strength. Cross-sectional dimensions often are governed by factors other than stress, such as minimum cover, so that the full strength capability of the concrete is not used. Further, the total prestress force that can be generated may not be sufficient to take advantage of the high strength concrete.

Other disadvantages of high strength concrete are its additional cost and the additional expenses of increased quality control. Finally, the AASHTO Specifications[8] tend to discourage the use of high strength concrete because the specifications are based on the properties of normal strength concrete.

APPLICATIONS OF HIGH STRENGTH CONCRETE

Solid Section Girders

The effect of using high strength concrete in four different solid section girders was investigated. Cross-sectional dimensions of the four girders—the bulb tee, the Washington State Department of Transportation (WSDOT) Standard, the AASHTO-PCI Standard Sections, and the Colorado Standard—are shown in Fig. 2. Two methods of attaching the decks were considered: integrally cast and cast in place. Decks were cast in place on the completed girder without shoring, so that the entire dead load of both girder and deck was carried by the girder section.

To determine span capabilities of the girders, AASHTO HS20-44 loading was used, with a lateral distribution factor S/5.5. Allowable stresses conformed to the AASHTO Specifications with allow-

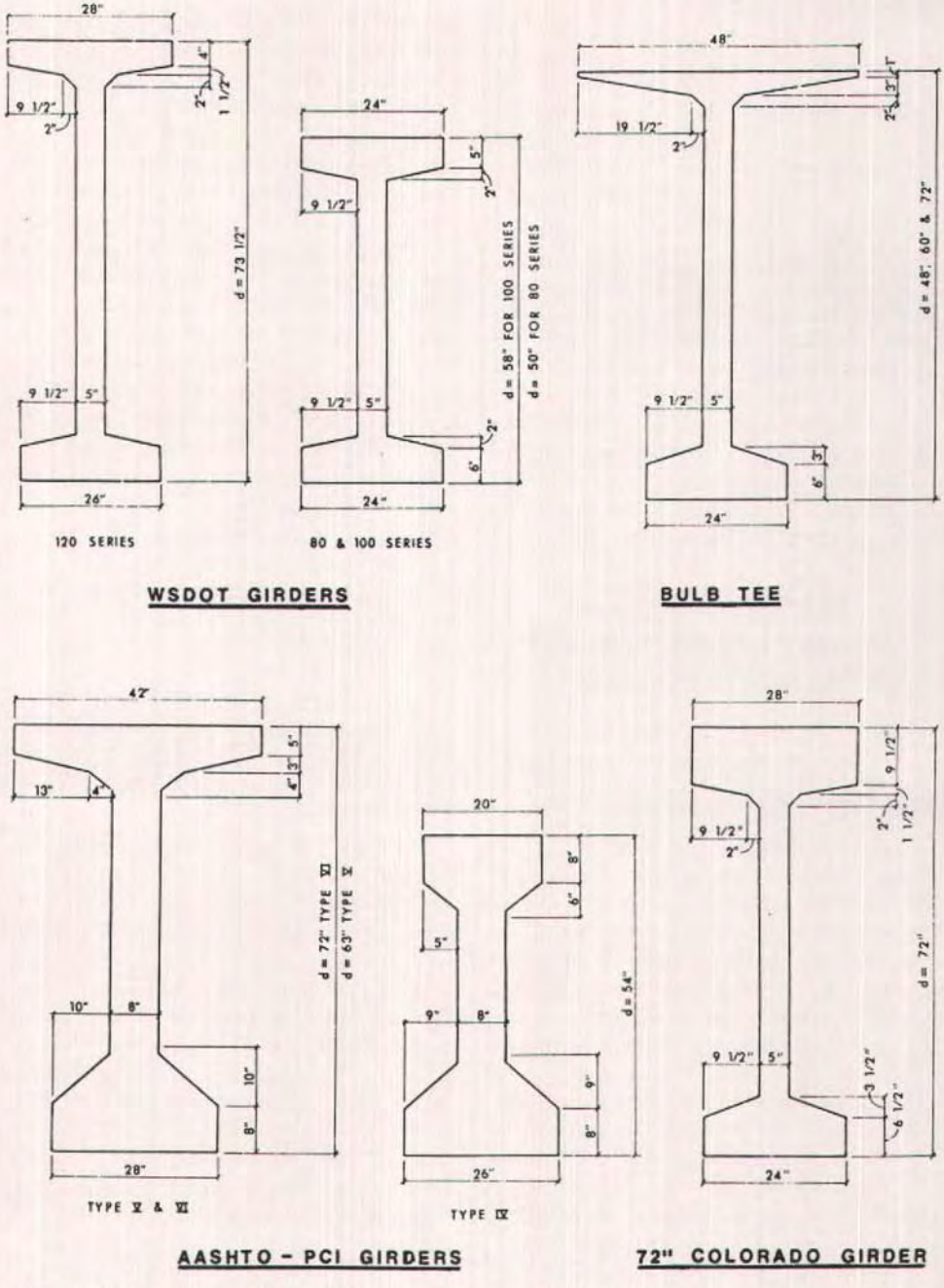

Fig. 2. Solid section girders — Cross sections investigated.

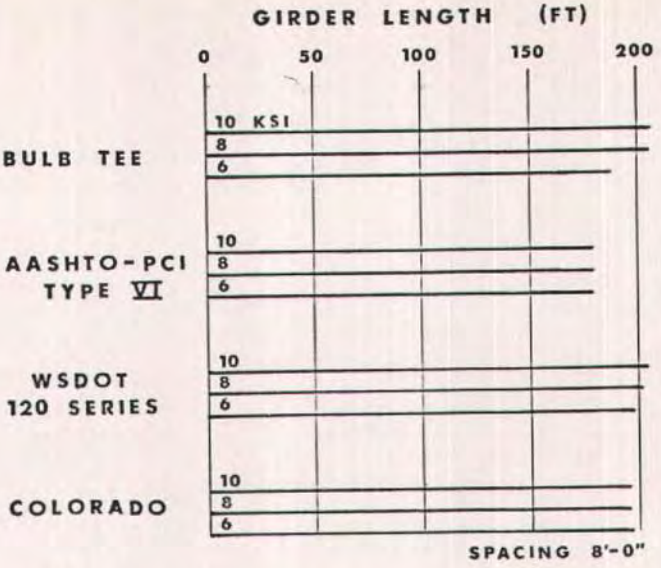

Fig. 3. Span capabilities — Basic 72-in. (1830 mm) sections with integral decks.

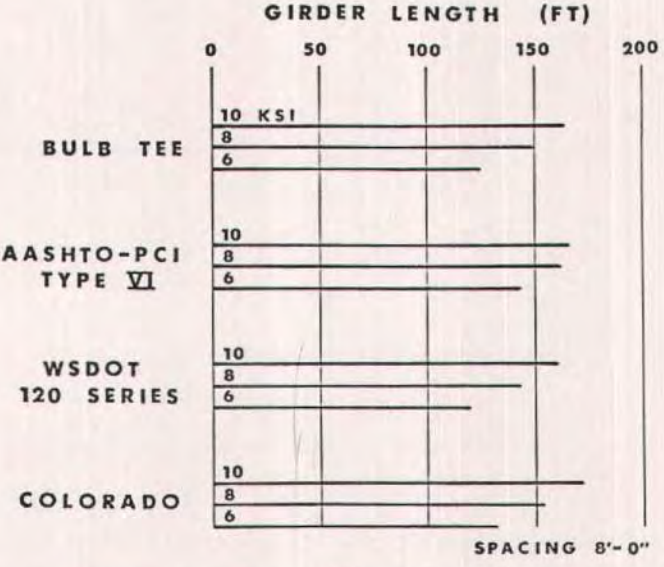

Fig. 4. Span capabilities — Basic 72-in. (1830 mm) sections with cast-in-place decks.

able tension in the precompressed tension zone equal to $3\sqrt{f'_c}$ ($0.249\sqrt{f'_c}$) and allowable compression equal to $0.4f'_c$.

The effectiveness of high strength concrete in increasing the span capabilities of a given cross section is shown in Fig. 3. Here, for a beam spacing of 8 ft (2.4 m), the span capabilities of all the basic 72-in. (1830 mm) deep integral deck sections are shown for the different

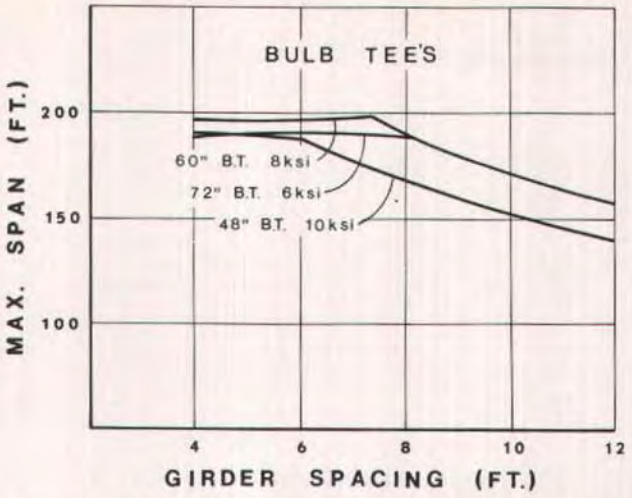

Fig. 5. Depth variations — Bulb tees with integral deck.

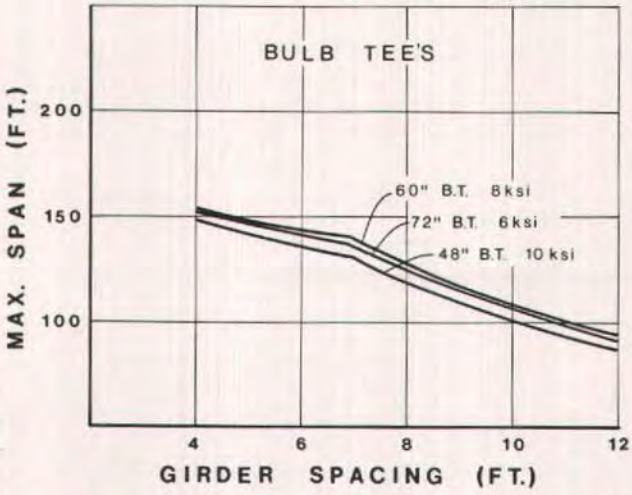

Fig. 6. Depth variations — Bulb tees with cast-in-place deck.

concrete strengths. The maximum available prestress force sets span length capabilities at the same value for all concrete strengths for the AASHTO-PCI and Colorado sections. However, for the bulb tee and WSDOT sections, the benefits of using high strength concrete are apparent.

The same information for the basic 72-in. (1830 mm) deep sections with cast-in-place decks is shown in Fig. 4. The benefits of high strength concrete in increasing span capabilities are easily identified, since the available prestress factor does not control.

A comparison of Figs. 3 and 4 shows the advantage of precasting the deck as an integral part of the beam section before prestressing. In addition to providing a high strength concrete in the deck,

the prestress force is extended into the compression flange resulting in greater span capabilities.

The potential for using shallower members with increasing concrete strength is shown in Figs. 5 and 6. For the integral deck, the potential for a reduction in depth from 72 to 48 in. (1830 to 1220 mm) is available for girder spacings up to 6 ft (1.8 m). The influence of maximum available prestress force limits the potential reduction for wider girder spacings. For the cast-in-place deck, the potential for reducing depth of section from 72 to 48 in. (1830 to 1220 mm) with an increase in concrete strength from 6 to 10 ksi (42 to 70 MPa) is available for all girder spacings.

Making maximum use of the greater load carrying capabilities of high strength concrete girders requires different designs for bridges. Two designs of a 150-ft (46 m) simple span bridge are shown in Fig. 7. On the left side, nine 6-ksi (42 MPa) concrete girders were used. On the right side, four 10-ksi (70 MPa) concrete girders were used. The advantages of the high strength concrete are evident: only four girders are needed for the high strength concrete design, while nine girders are needed for the normal strength concrete design. Despite the thicker cast-in-place deck needed for the greater transverse span between the four girders, the overall dead load is reduced, and therefore total prestressing requirements are reduced.

Post-Tensioned Box Girders

Multiple span, cast-in-place, continuous post-tensioned box girder bridges of constant depth were represented by the two-span continuous structure shown in Fig. 8. Concrete strengths were 6, 8, and 10 ksi (42, 56, and 70 MPa). Overall beam depths were 4.5, 5.5, and 6.5 ft (1.4, 1.7, and 2 m). Allowable stresses were the same as those used in the solid section girder analysis, except that allowable tension in the precompressed tension zone was assumed to be $6\sqrt{f'_c}$ ($0.498\sqrt{f'_c}$). Loading was three lanes of AASHTO HS20-44, without lane reduction.

Span capabilities for the different girder depths are shown in Fig. 9. High strength concrete for continuous box girders of 150 to 250 ft (46 to 76 m) spans increased span capabilities. As with the integral deck solid section girders, the maximum available prestress force limited capabilities of the high strength concrete.

Segmentally Post-Tensioned Box Girders

Segmentally post-tensioned box girder bridges of medium to long span were represented by the free cantilever Shubenacadie Bridge (South Mainland, Nova Scotia) with a 700-ft (213 m) main span and 372-ft (113 m) side spans.[10] Overall dimensions of the bridge are shown in Fig. 10. The bridge was constructed with 5-ksi (35 MPa) concrete and used 1.25-in. (31.75 mm) diameter thread bars for post-tensioning. No tension was allowed in the precompressed tension zone. AASHTO HS20-44 loading was used.

The bridge was reanalyzed using 10,000-psi (70 MPa) concrete to determine how much the thickness of the lower flange could be reduced and what effect this reduction would have on the overall moments. As shown in Fig. 11, using high strength concrete reduced the total flexural prestress force by more than 10 percent as a result of the reduced dead load. The optimum lower flange thickness is 1.6 ft (0.5 m), obtained at about 8-ksi (56 MPa) strength.

For segmentally post-tensioned box girder bridges, high strength concrete is feasible in regions, such as the lower flange, where the design is controlled by stress. In regions such as in the deck, where the design is controlled by other factors, normal strength concrete can be used. The webs may be constructed of either high strength concrete or normal strength concrete, depending on mini-

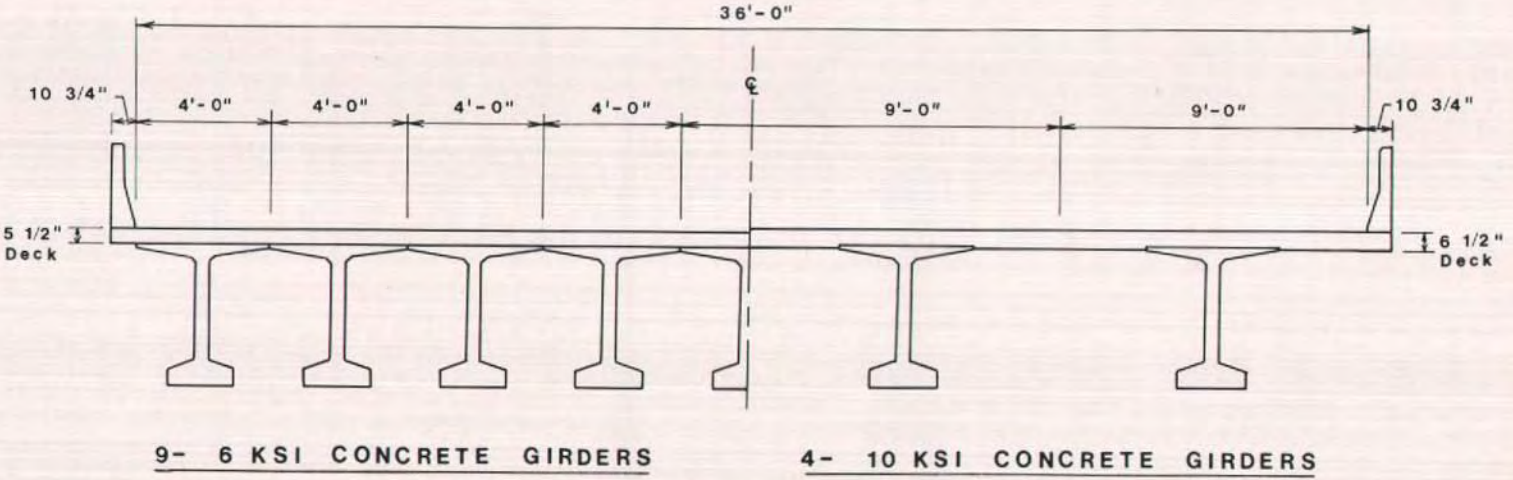

Fig. 7. Comparison of cross section designs of a 150-ft (45.7 m) simple span bridge made possible by using alternate concrete strengths.

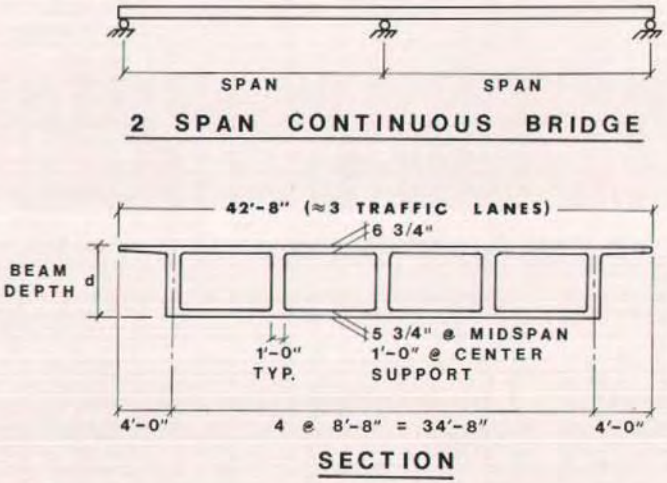

Fig. 8. Two-span continuous post-tensioned box girder bridge.

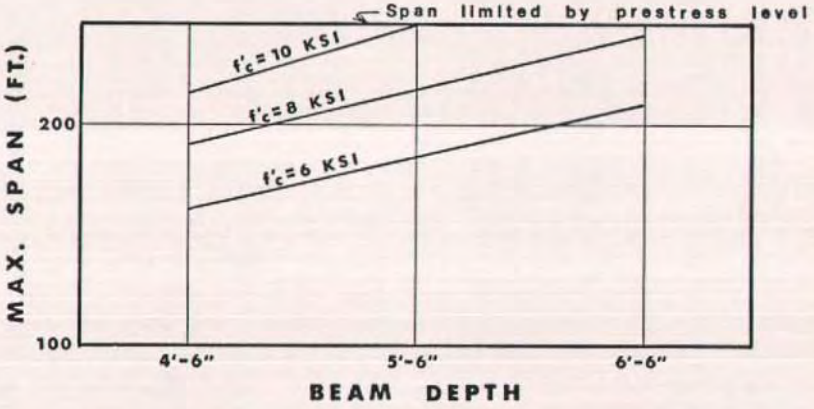

Fig. 9. Span capabilities — Two-span continuous box girder bridge.

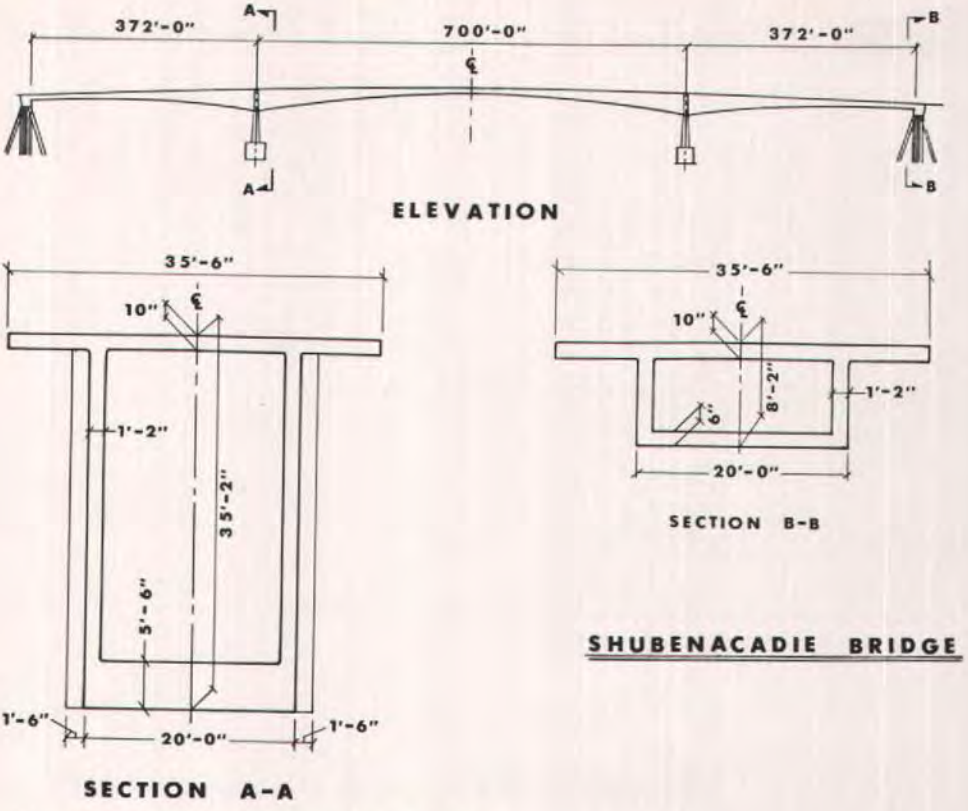

Fig. 10. Shubenacadie free cantilever bridge.

mum thickness requirements, minimum shear reinforcement requirements, and the contribution of concrete in the webs to the shear carrying capacity.

Compression Members

Solid pier shafts and elements of Y-piers (Fig. 12) are examples of compression members in bridges. Compression members were expected to benefit greatly from applications of high strength concrete.

To study the effect of increasing the compressive strength of concrete from 6 to 10 ksi (42 to 70 MPa), interaction diagrams were developed for the compression strut shown in Fig. 13. The diagrams were developed for a pin end condition, assuming that the cross section possessed the bilinear moment-curvature relationship defined by strain compatibility and the elastic properties of the concrete and prestressing strand. The deflected shapes were determined by integrating the curvatures along the length of the member. The ultimate strength design method was used with factored loads.

Fig. 14 shows that capacities of the compression strut increase with increases in concrete strength.

Results of the compression member study are shown in Table 1. Three slenderness ratios, three concrete strengths, and three eccentricities are shown. For short, concentrically loaded struts, ca-

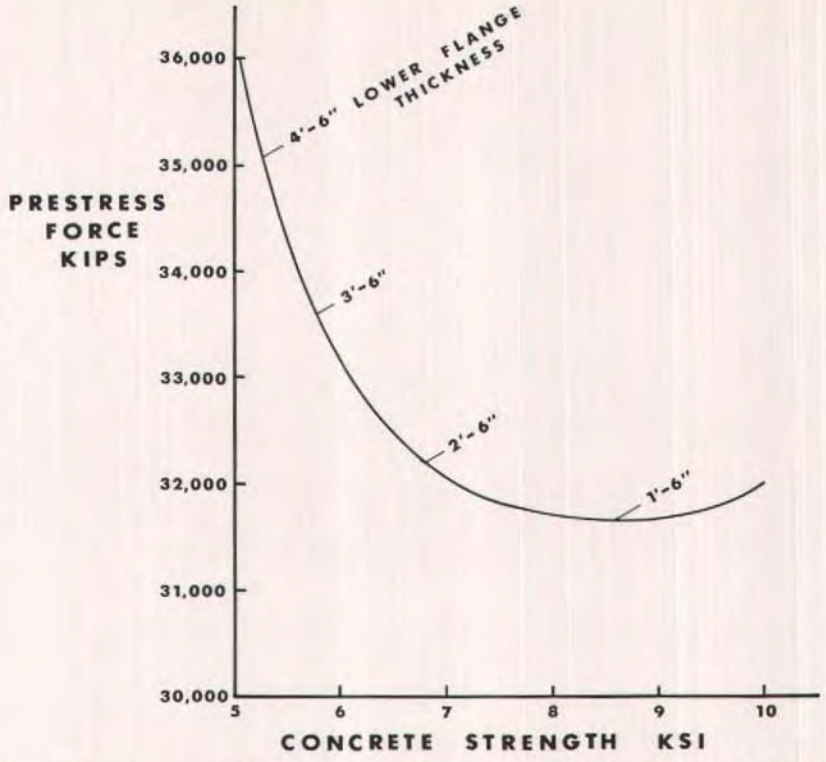

Fig. 11. Variation of prestress force and flange thickness with concrete strength — Shubenacadie Bridge.

Table 1. Axial load capacities for 10-in. (254 mm) square strut.

		Eccentricity					
		$e=0$		$e=0.1D$		$e=0.2D$	
l/r	f'_c (ksi)	P (kips)	P/P_o	P (kips)	P/P_o	P (kips)	P/P_o
0	6	375	1.00	284	1.00	217	1.00
	8	518	1.38	389	1.37	294	1.35
	10	662	1.77	478	1.69	362	1.67
50	6	320	1.00	233	1.00	168	1.00
	8	437	1.37	317	1.36	220	1.31
	10	545	1.70	390	1.67	267	1.59
100	6	205	1.00	133	1.00	80	1.00
	8	270	1.32	165	1.24	90	1.13
	10	325	1.59	190	1.43	100	1.25

Note: ϕ factors P in accordance with ACI 318-77, Section 9.3.2c,[9] and AASHTO Specification, Section 1.5.33.4,[8] are included in this table.

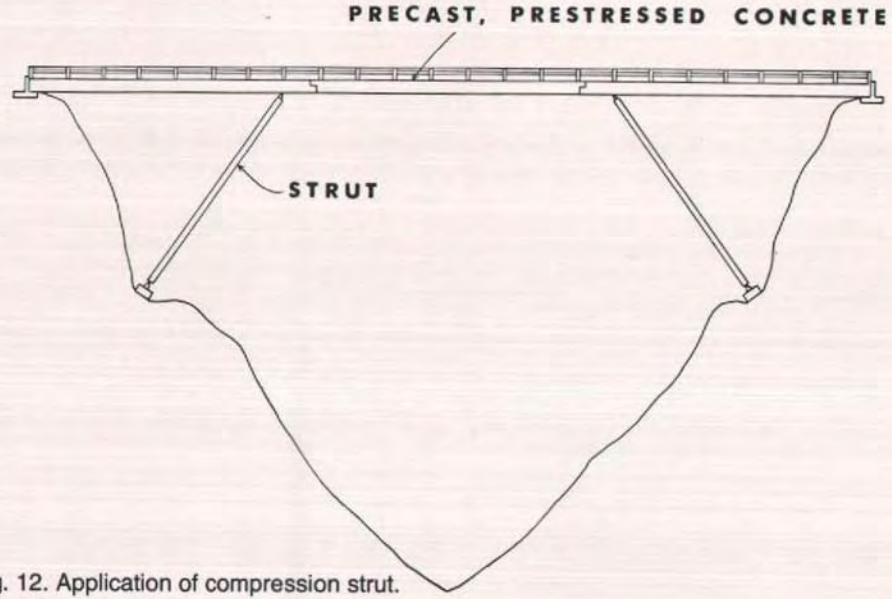

Fig. 12. Application of compression strut.

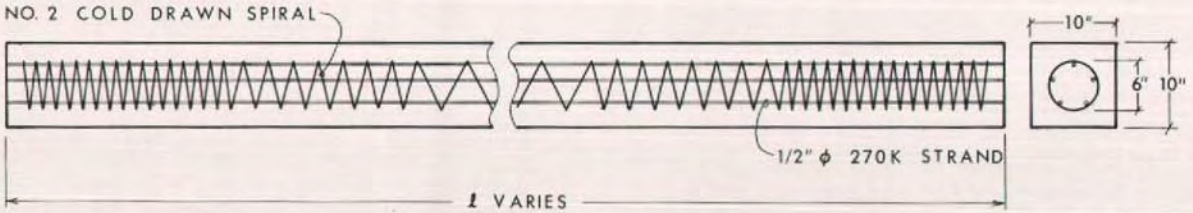

Fig. 13. Strut details.

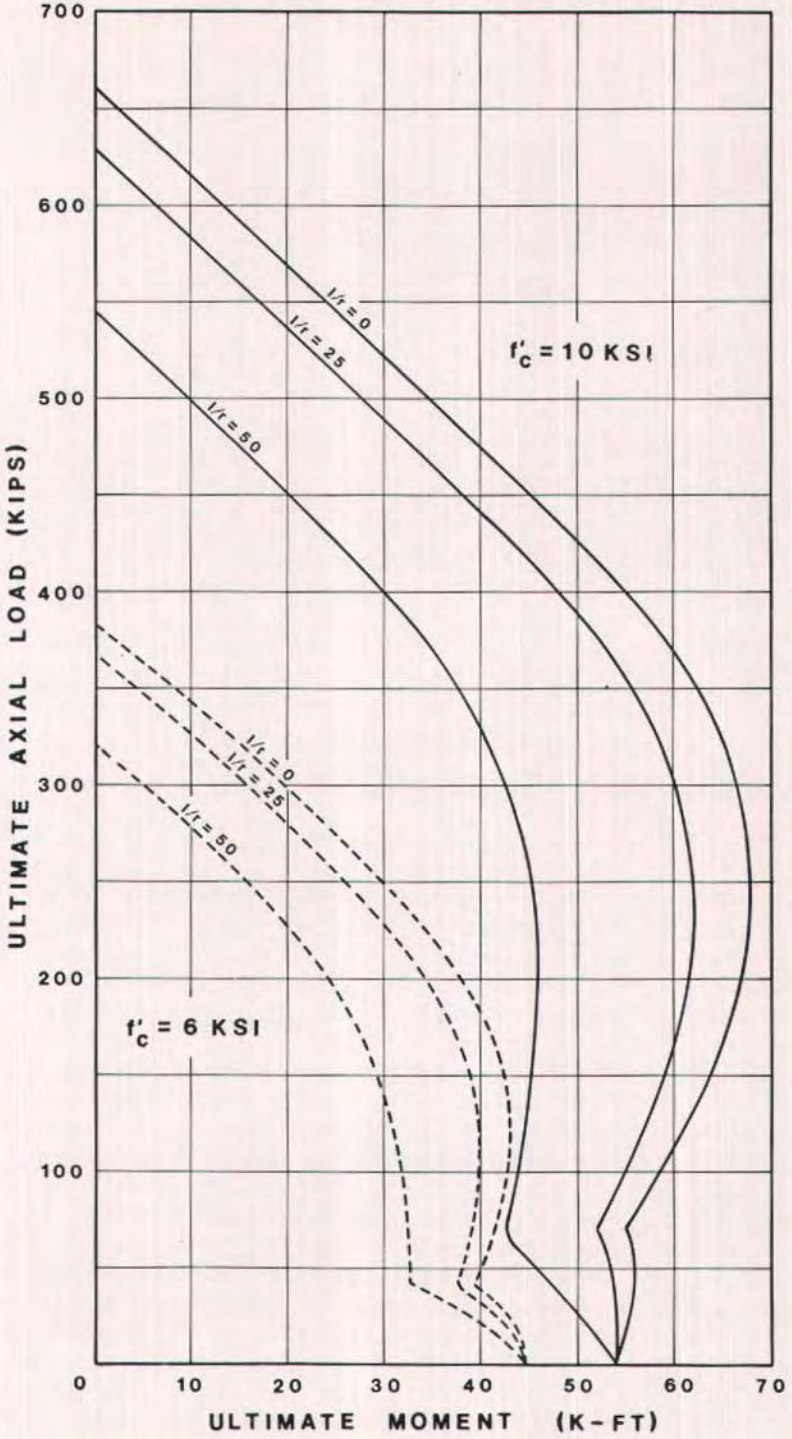

Fig. 14. Interaction diagram — 10 in. (254 mm) square prestressed strut.

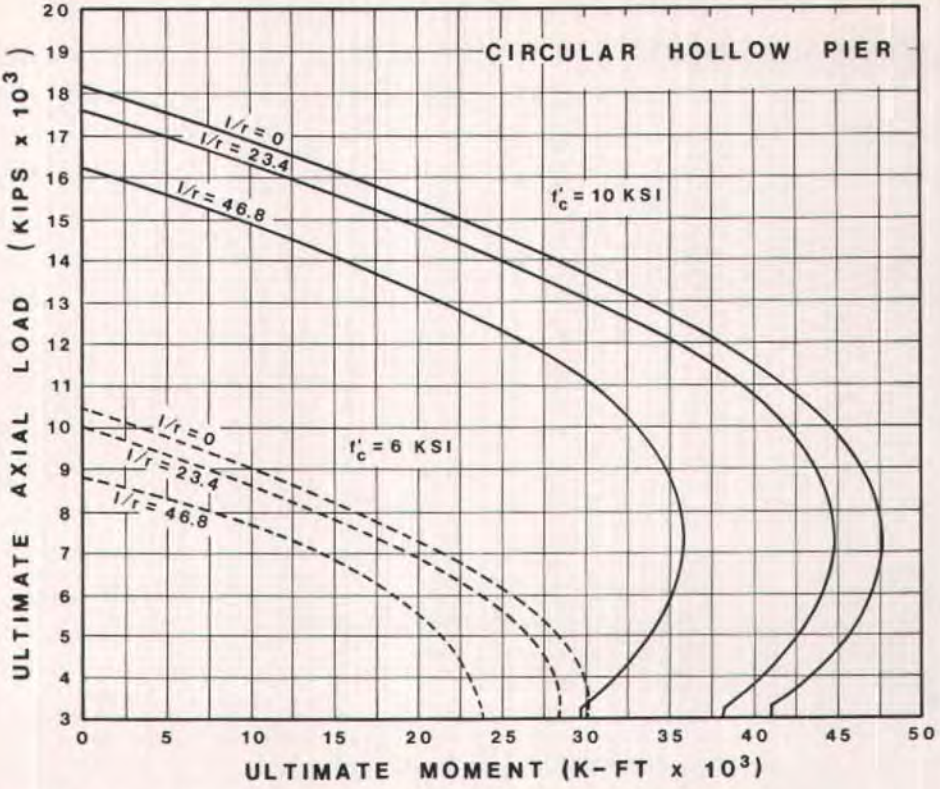

Fig. 15. Interaction diagram — 15 ft (4.57 m) diameter circular hollow pier.

pacity is determined by multiplying the cylinder strength by the cross-sectional area and then subtracting the prestress force. Because the prestress force is constant, the benefits of increasing concrete stength are more than the strength increase itself. This is illustrated by the strength ratios in the table that exceed 10/6 = 1.67 for those struts.

For combined axial load and bending, using high strength concrete even for relatively slender columns is beneficial. It can be concluded that compression members are an excellent application for high strength concrete. Smaller sections can be used for a given number of members, or fewer members can be used in a given location. In either case, weight as well as material and construction cost are reduced.

Thin Walled Sections

A circular and a square pier with 6-in. (152 mm) wall thicknesses were chosen for investigation. A 15-ft (4.6 m) outside diameter hollow circular pier had a prestress steel area of 20.2 sq in. (130 cm²). A 10-ft (3 m) square hollow pier had a prestress steel area of 18.4 sq in. (118 cm²) concentrated in the corners. Concrete strengths studied were 6 and 10 ksi (42 and 70 MPa).

The piers were considered to have pinned end connections which were free to rotate but not free to translate. The 1977 AASHTO Specifications, Section 1.5-31,[8] were used to design the piers. Interaction diagrams were constructed using the assumption that the concrete stress equal to 0.85 f'_c was dis-

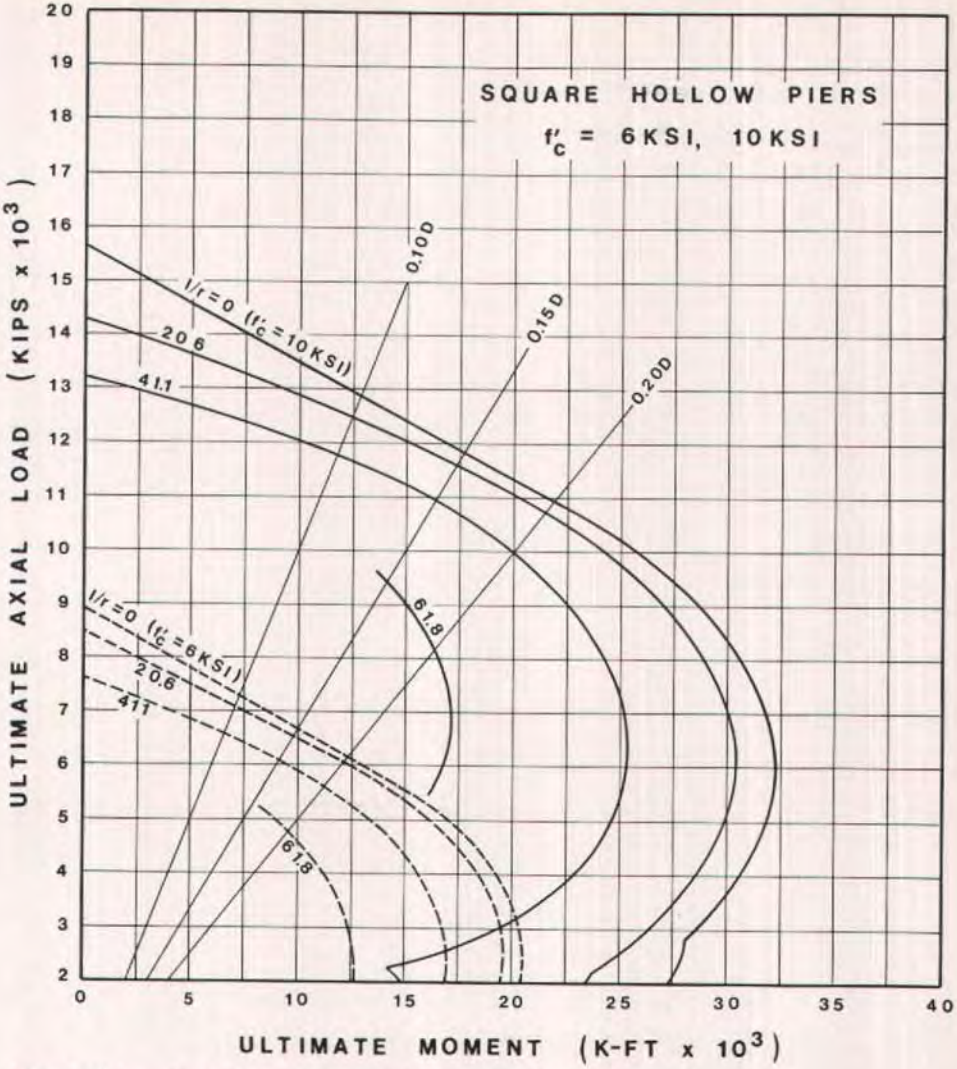

Fig. 16. Interaction diagrams — 10 ft (3.05 m) square hollow pier.

tributed as a rectangular stress block. A bilinear moment-curvature relationship was used to approximate the actual parabolic moment-curvature of the section. The final deflected shape of the column from which the information for the interaction diagram was obtained was constructed using the same principles as outlined for compression struts. Concrete stresses were obtained from the parabolic stress-strain curve for the concrete, assuming a maximum strain of 0.003. From the column-deflection curves, a combination of eccentricity of axial load and height of column is found for a particular axial load. A range of axial loads were considered from zero to the case of pure compression.

The interaction diagrams in Fig. 15 and in Fig. 16 show the increased capacity of the piers when concrete strength is increased from 6 to 10 ksi (42

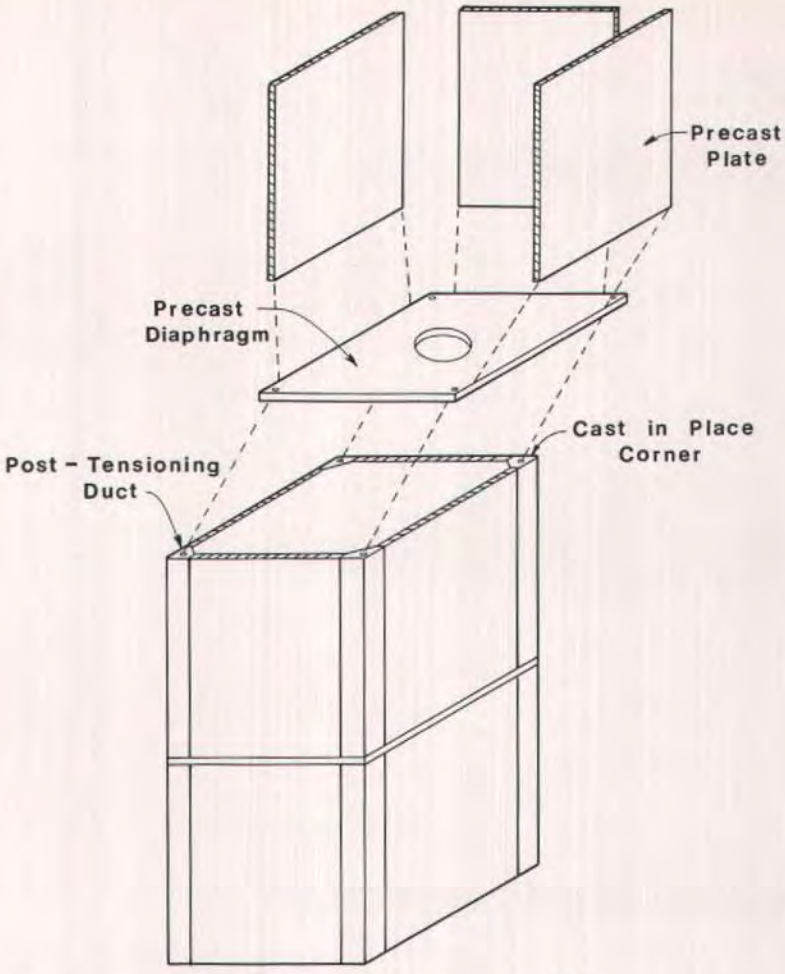

Fig. 17. Square hollow pier — Thin plate precast segments.

to 70 MPa). The benefit of increasing concrete strength is more than directly proportional to the strength increase.

High strength concrete permits the adaptation of thin wall members to pier construction for major bridge spans. The strength of these sections permits their use when tall piers are required. The increased load carrying capability permits longer spans or fewer piers. The lighter section permits construction with minimal disruption to surrounding terrain.

Two construction procedures are shown in Figs. 17 and 18. In Fig. 17, thin plates are joined at the corners with cast-in-place concrete. By building the piers out of sections of plates and installing the precast diaphragms shown at 5 to 10 ft (1.5 to 3 m) levels, these plates could be erected with the utilization of a gin pole and minimum winch capacity.

In Fig. 18, the square prismatic box sections are match cast, transported to the site, and post-tensioned to form the pier using standard segmental construction methods. The size of the sections could be controlled by site requirements and crane capacities.

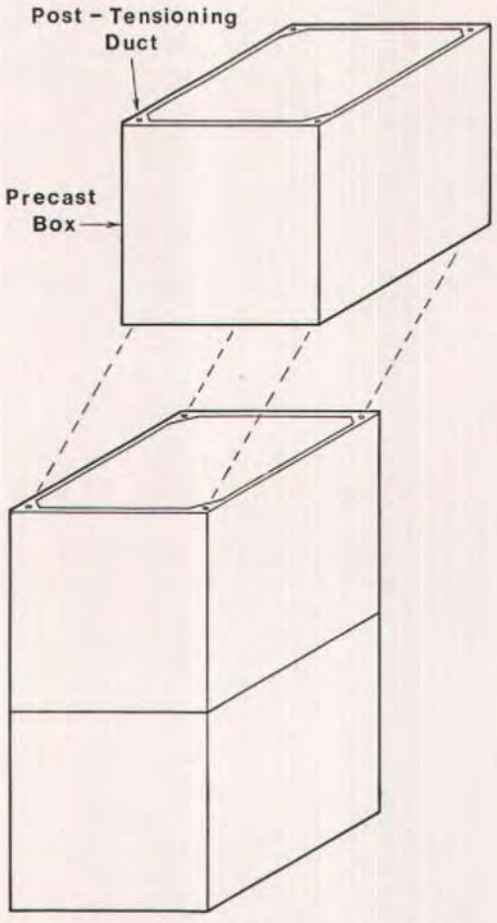

Fig. 18. Square hollow pier — Match cast precast segments.

Evaluation of Benefits

The results of the study of applications of high strength concrete to bridge members are evaluated qualitatively in terms of a number of criteria listed in Table 2. Struts and hollow piers offer the best possibility for materials savings percentage-wise over the other members since either the sizes of the individual members or the total number of members can be reduced. The potential for reduced shipping weight for hollow pier prismatic members or plates offers a relatively new construction procedure for this bridge member. These precast sections can be adapted to changing requirements by form modification if the change is not major. These factors led to the selection of a test program for square hollow piers.

DESIGN OF TEST SPECIMEN

Objective

A square hollow pier specimen was selected to determine that design could

Table 2. Evaluation of benefits of using high strength concrete.

Member or system	Materials savings	Reduced shipping weight	Reduced structure depth	Difficulty of production	Adaptable standard section
Solid section girder, integral deck	Medium	Medium	High	Medium	Medium
Solid section girder, cast-in-place deck	Medium	Medium	High	Medium	Medium
Commonly used box girders	Medium	—	High	High	Low
Segmentally post-tensioned box girders					
Plant precast	Medium	High	Medium	Medium	—
Cast-in-place	Medium	—	Medium	High	—
Struts, solid square	Medium	High	—	Low	High
Piers, hollow thin walled	Medium	High	—	Medium	High

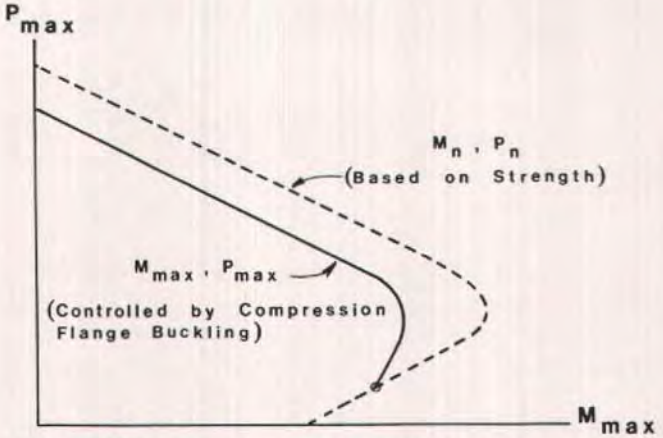

Fig. 19. Interaction diagram — Thin plate buckling.

be controlled by overall buckling of the pier rather than by buckling of the thin plate wall of the pier. Fabrication procedures for thin plate segments with cast-in-place corners would be compared with plant fabricated match cast prismatic boxes. Post-tensioned construction techniques would be confirmed.

Analytical Development

Although studies of thin plate buckling of steel plates have been made, the application of these studies to concrete

thin plates was questionable. Applying formulas developed by Priest[11] for high strength steels and using these formulas with k factors suggested by Bleich[12] for buckling strength of metal structures results in:

$$\sigma_{cr} = \frac{\pi^2 E_t}{3(1-\mu^2)}\left(\frac{t}{b}\right)^2 \qquad (1)$$

in which

σ_{cr} = critical unit compressive stress, psi
E_t = tangent modulus of elasticity, psi
μ = Poisson's ratio
b = width of plate, in.
t = thickness of plate, in.

As can be seen from Eq. (1), the critical stress is directly proportional to the modulus of elasticity and to the square of the thickness-to-width ratio of the plate.

In applying this equation to hollow rectangular piers, the following comments can be made:

1. Under concentric axial load where the entire section is subject to uniform compression, all four sides of the cross section are equally susceptible to buckling.

2. When the section is subject to eccentric load, the compression flange will be the most likely to buckle first.

3. Considering that only eccentric loads are encountered in practical applications, local buckling of the thin compression flange should be considered in the capacity investigation of the section.

4. An interaction diagram that will take compression flange stability as well as overall stability into consideration in addition to material failure appears to represent the only logical solution to the problem.

Fig. 19 shows a schematic of such an interaction diagram. Note that the ACI Code[9] concrete stress block cannot be used to develop this diagram. Instead, representative stress-strain diagrams, as shown by Fig. 20, must be used in the computation. In determining critical stress, average rather than maximum stress in the compression flange should be used.

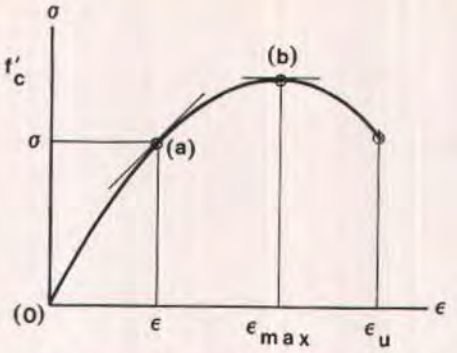

Fig. 20. Typical concrete stress-strain curve.

The comprehensive interaction diagram shown in Fig. 19 will handle any buckling situation for square or rectangular piers. A computer program written in Fortran IV language was prepared for this project enabling the analysis of hollow rectangular concrete sections containing prestressed and nonprestressed reinforcement.

Interaction diagrams developed from this program for 10-ft (3 m) square hollow piers with 3, 4, 5, and 6 in. (76, 102, 127, and 152 mm) wall thicknesses are shown in Fig. 21. In order to show the effect of local buckling of the compression flange on the load resistance of the cross section, curves representing load capacities based on both material failure and local buckling are portrayed. An examination of the figure indicates that the gap between capacity based on material failure and that controlled by local buckling increased with the decrease of the thickness-to-width ratio of the compression flange.

SQUARE HOLLOW PIER TEST SPECIMEN

A 5-ft (1.5 m) square cross section member with a 1½-in. (40 mm) thick

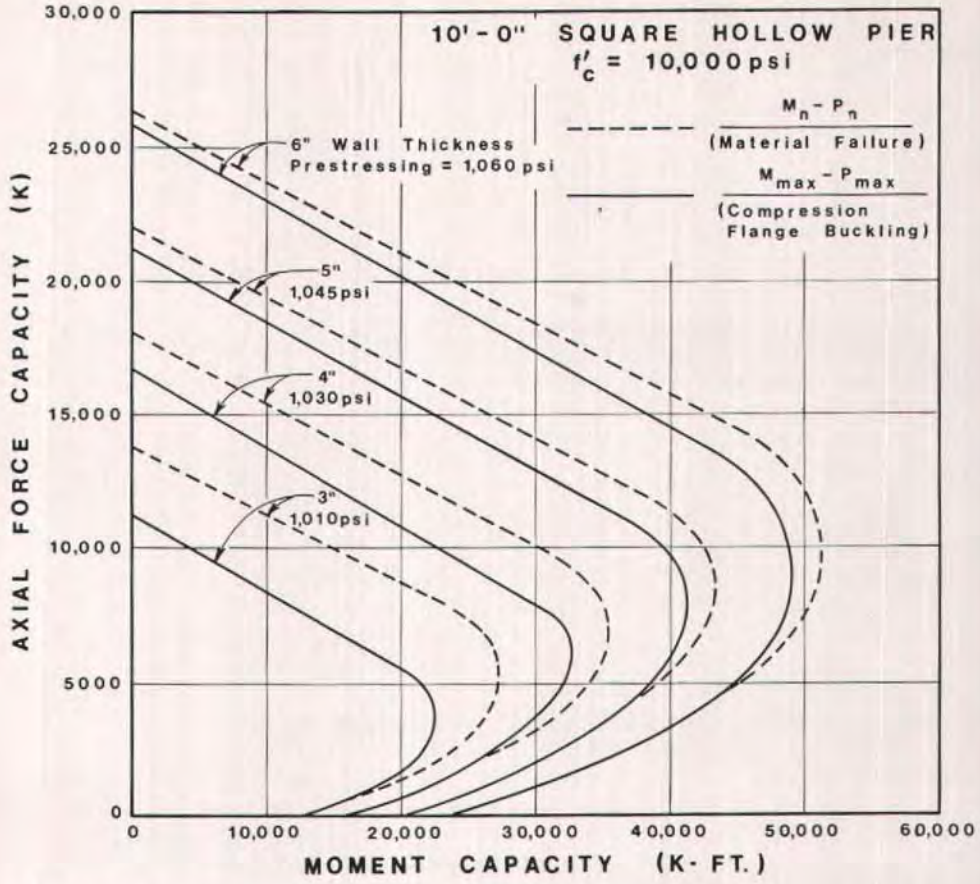

Fig. 21. Interaction diagram for a 10-ft (3.05 m) square hollow pier.

wall was selected as representative of a half-scale model of a 10-ft (3 m) square pier with 3-in. (76 mm) wall thicknesses as shown in Fig. 22. A 15-ft (4 m) length was selected to provide short column action removing the parameter of overall pier stability.

The interaction diagram for the specimen is shown in Fig. 23. The predicted test results based on the specimen performing in accordance with the theory developed are tabulated in Table 3.

Fabrication of Test Specimens

Match cast precast segments 5 ft (1.5 m) square with 5 ft (1.5 m) long and 1½-in. (40 mm) thick walls were selected for testing. As shown in Fig. 24, three segments would be match cast and connected together by post-tensioning, making a 15-ft (4.6 m) long pier to be tested for local buckling. The match cast forming is shown in Fig. 25. Specimens were cast in the architectural plant at Concrete Technology Corporation, epoxied and tensioned together, and moved into the laboratory as shown in Fig. 26.

The fabrication procedures confirmed the difficulties that could be experienced in match casting square boxes with thin walls. It was found to be dif-

Table 3. Predicted test results.

e (in.)	P (kips)	M (kip-ft)	Curvature (rad/in.)	Deflection (in.)	End rotation (degrees)
6	2300	1150	1.041×10^{-5}	0.04	0° 3'14"
12	1890	1890	1.46×10^{-5}	0.06	0° 4'32"
24	1390	2780	2.01×10^{-5}	0.08	0° 6'14"
36	990	2970	3.43×10^{-5}	0.14	0° 10'36"

ficult to maintain the alignment of the walls. Furthermore, the thin sections created a problem in placing high strength concrete with the necessary slump requirements into the thin section. A preferable construction would be to cast thin plates on a continuous bed as is customary in precasting plants, truck them to the site on flatbed trucks, erect them in position and cast corners in place with longitudinal post-tensioning.

Testing Procedures

The test arrangement is shown in Fig. 27. Loading rams were located to provide the necessary eccentricities for the specimens as required in Table 3. Loading was applied in two phases. The first load phase was planned to study the performance of the specimen under service load conditions by cycling the load in small increments from zero to service load level. The second load phase was planned to verify the ultimate load capacity of the specimen as well as the mode of failure. The load was applied in small increments from service load to failure load.

Instrumentation included load cells for measuring forces, potentiometers for measuring displacements and curvatures, and strain gages for measuring strain in concrete. Experimental information was recorded using a high speed automatic data acquisition system. The load cell arrangement for Specimen 1 is shown in Fig. 28.

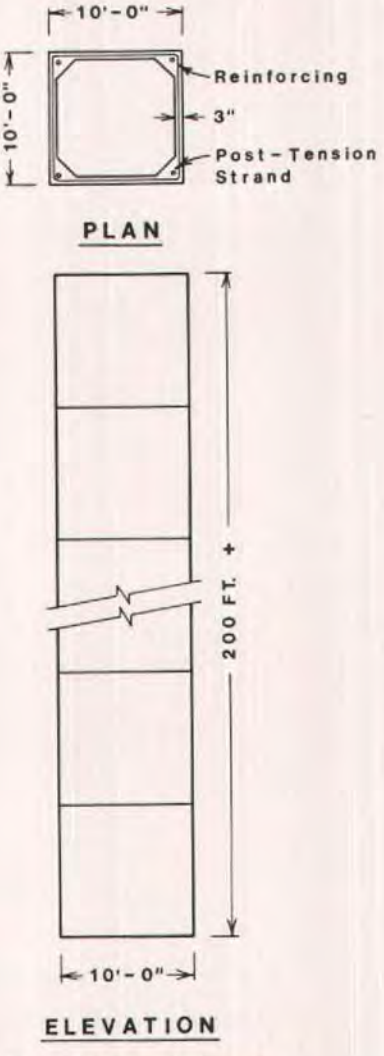

Fig. 22. Square hollow pier.

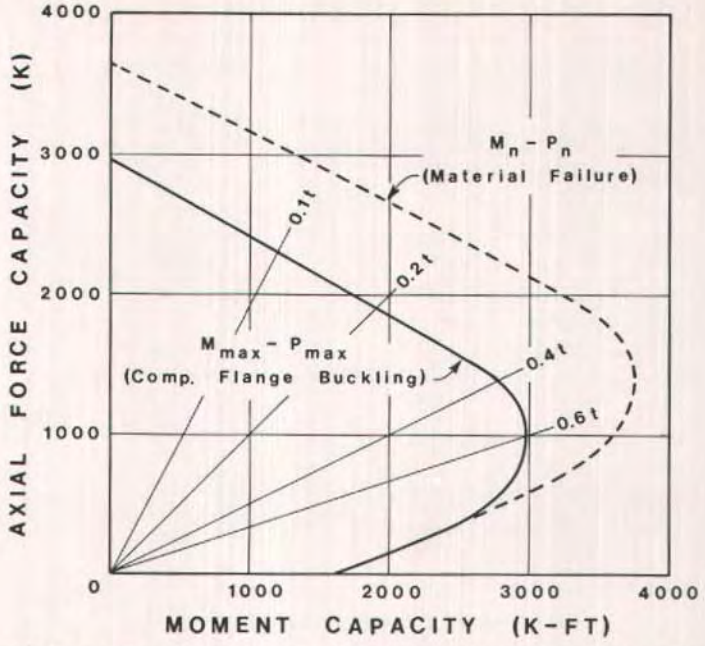

Fig. 23. Interaction diagram — 5 ft (1.52 m) square hollow pier specimen.

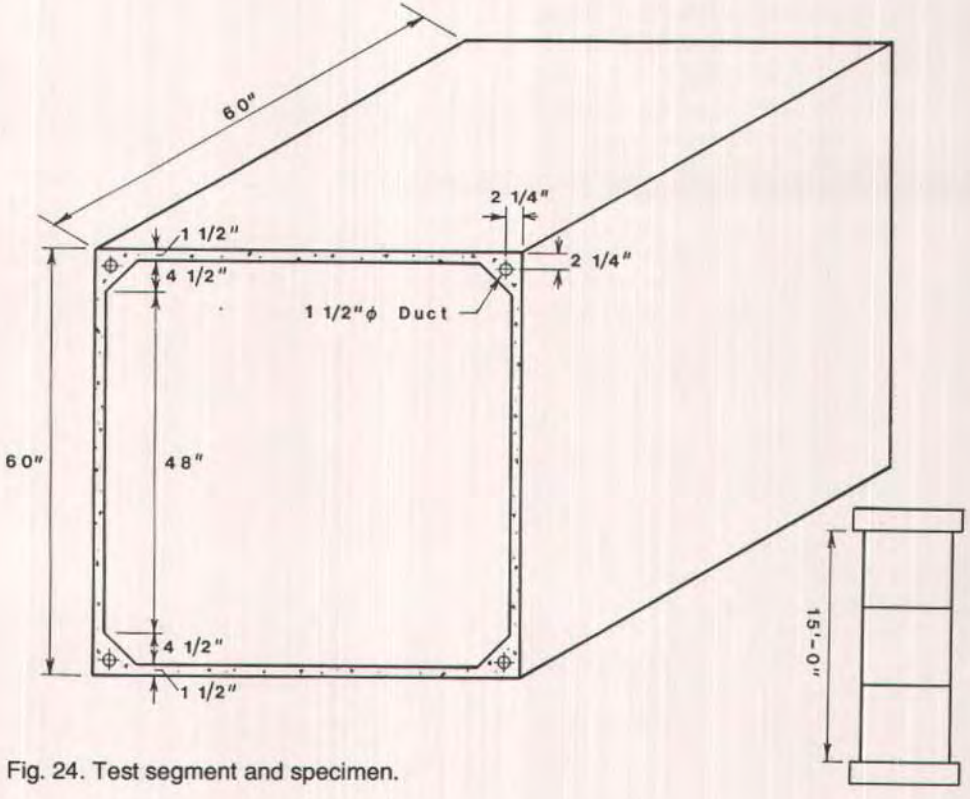

Fig. 24. Test segment and specimen.

Fig. 25. Forming of match-cast segment which was post-tensioned to adjoining segments before being moved to the testing lab.

Analysis of Test Data

Loading was applied to Specimen 1 to place the total reaction of all loads at a 6-in. (152 mm) eccentricity. The specimen failed explosively in the center segment at a load of 1,613,500 lbs (7172 kN) at an eccentricity of 4.9 in. (124 mm). Fig. 29 shows the buckling of the top plate. The failure extended totally through the specimen at approximately the same location. The concrete strength in the failed segment at the time of testing was 8680 psi (60 MPa). An interaction diagram based on this strength is shown in Fig. 30. The failure point indicated on the diagram shows that the actual failure load is reasonably close to the predicted envelope.

Specimen 2A was loaded at an eccentricity of 20 in. (508 mm). It failed explosively like Specimen 1 at a load of 1,346,000 lbs (5983 kN) at an eccentricity of 20.2 in. (513 mm). The failed specimen is shown in Fig. 31. The compressive strength for Segment 6A at time of failure was 9880 psi (68 MPa). The in-

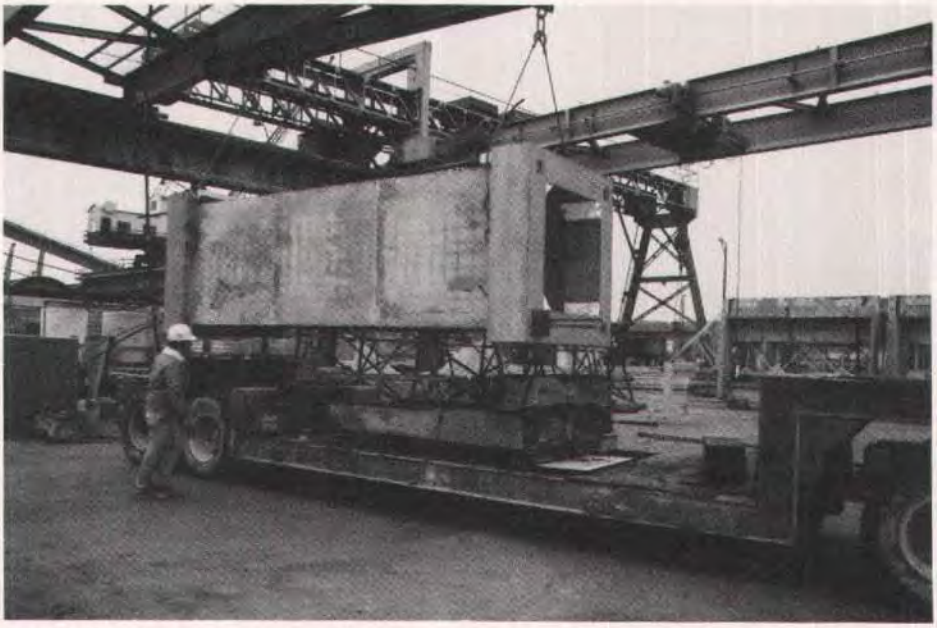

Fig. 26. Specimen being moved from precasting plant to testing lab.

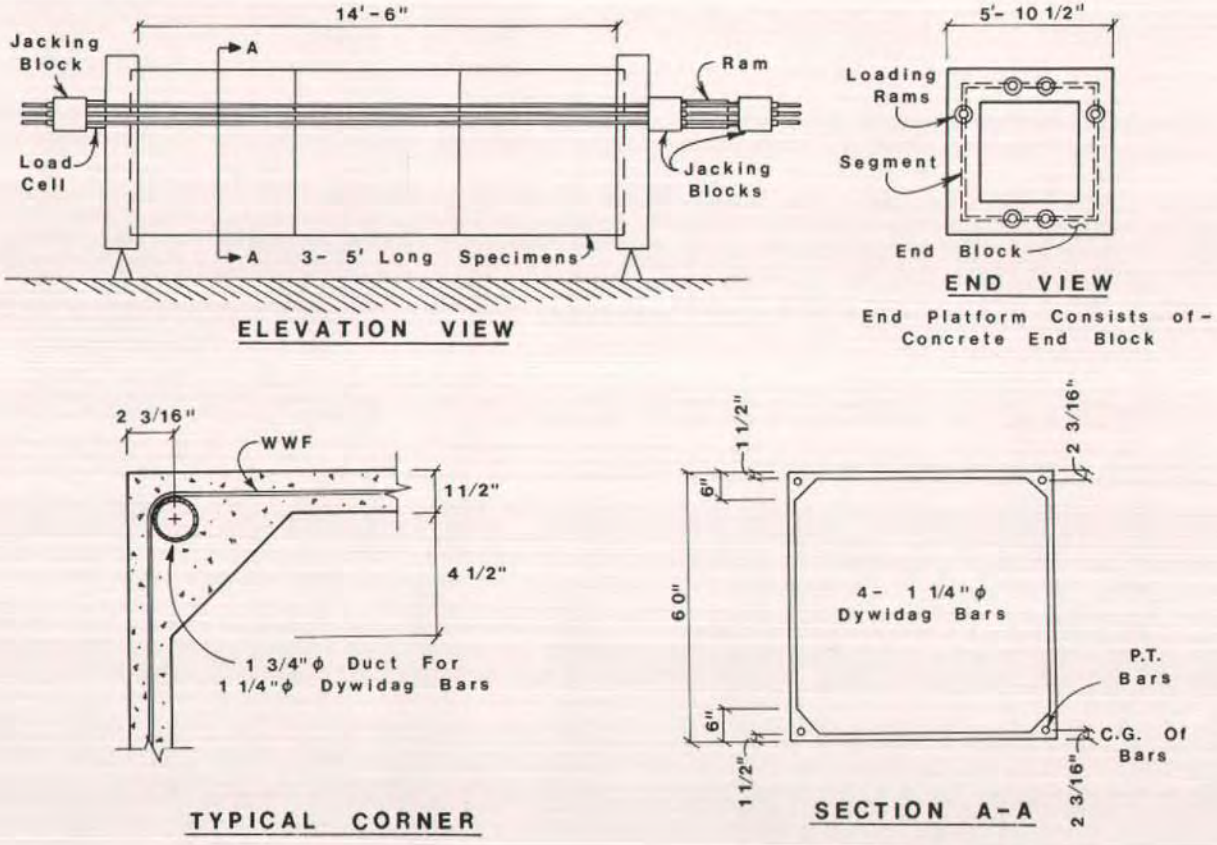

Fig. 27. Square hollow pier test arrangement.

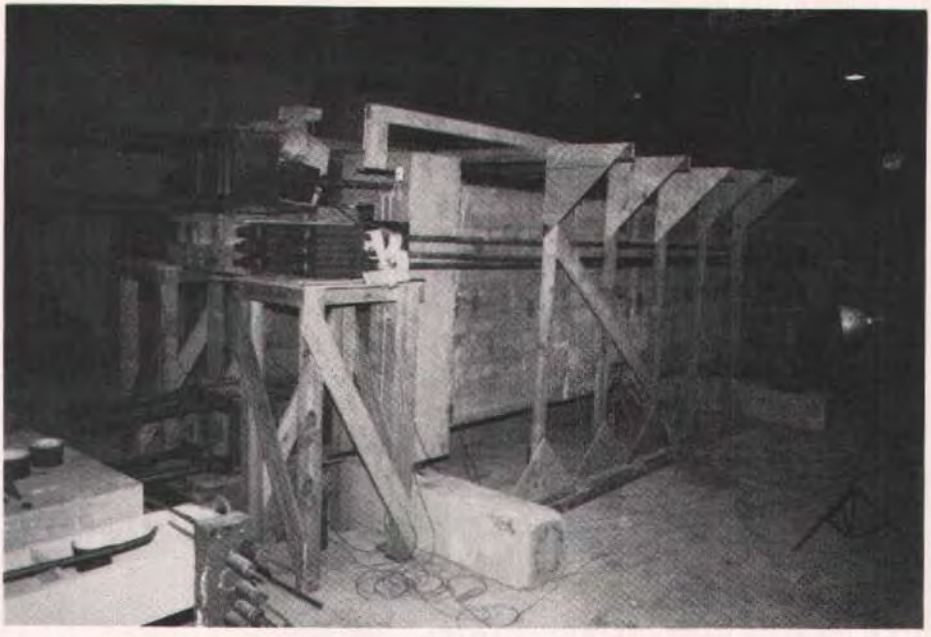

Fig. 28. Load cell arrangement for Specimen 1.

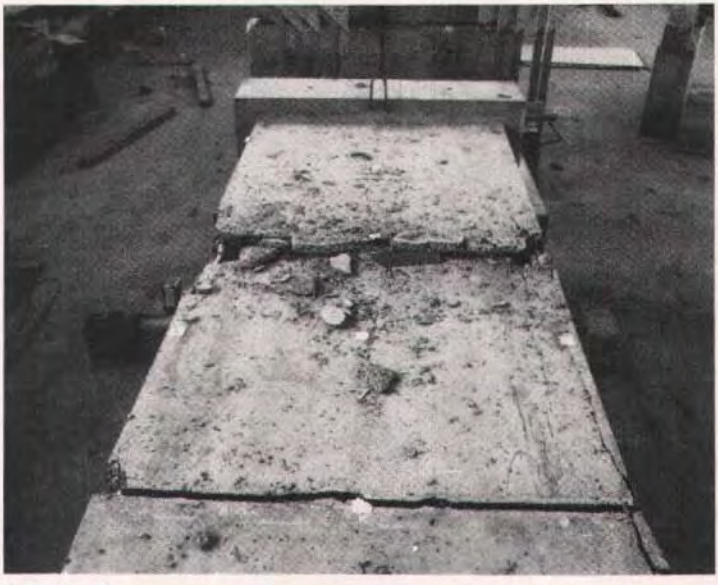

Fig. 29. Specimen 1 — Top plate — View of top plate looking west showing buckling of west plate over east plate. Diagram at right shows orientation of specimen and location of failure.

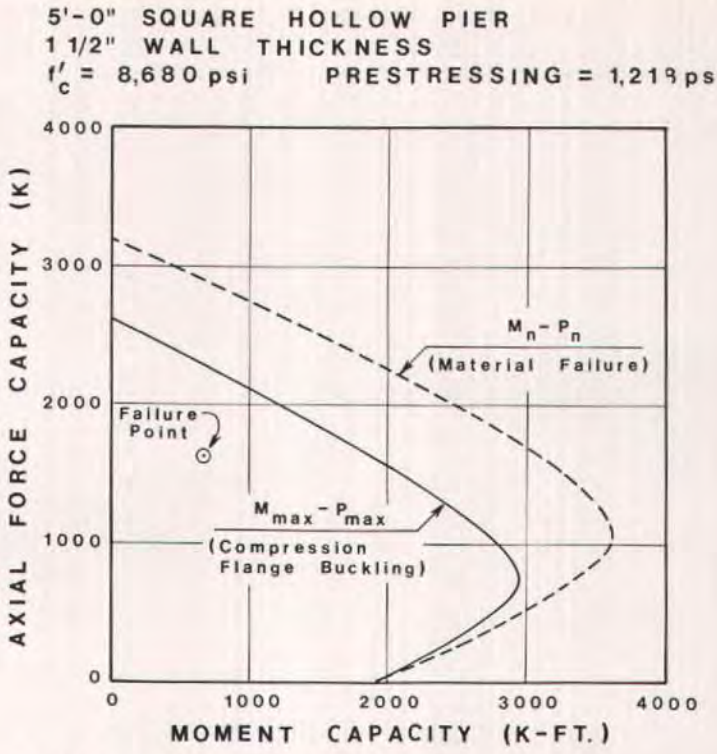

Fig. 30. Specimen 1 — Interaction diagram.

teraction diagram shown in Fig. 32 for 10,000-psi (70 MPa) concrete shows the failure point. Once again, the failure load is very close to the predicted failure envelope. These two specimens confirmed two points in the interaction diagram at widely separated eccentricities.

The two points are on the flat portion of the diagram which are points of critical concern in most pier failures. Therefore, this data can be considered adequate as a verification of that portion of the diagram. Testing of additional specimens at eccentricities between the two tested would serve as additional confirmation of the straight portion of the diagram. When eccentricities are great enough to cause tension in the bottom plate, the interaction diagram closes rapidly to the point where overall stability and local plate buckling are approximately equal. Therefore, this condition is not crucial; however, an additional test at the apex of the curve is recommended.

CODE PROVISIONS

Requirements such as minimum steel and concrete cover limit the thinness of plates used in bridge construction to a condition where thin plate buckling generally is not a problem. Thin sections are not considered due to durability and impact concerns. Therefore, criteria for concrete thin plate buckling are not included in the current codes. With the advent of high quality dense concrete, these limitations have the potential of being removed, which would then require the incorporation of buckling criteria into codes of practice.

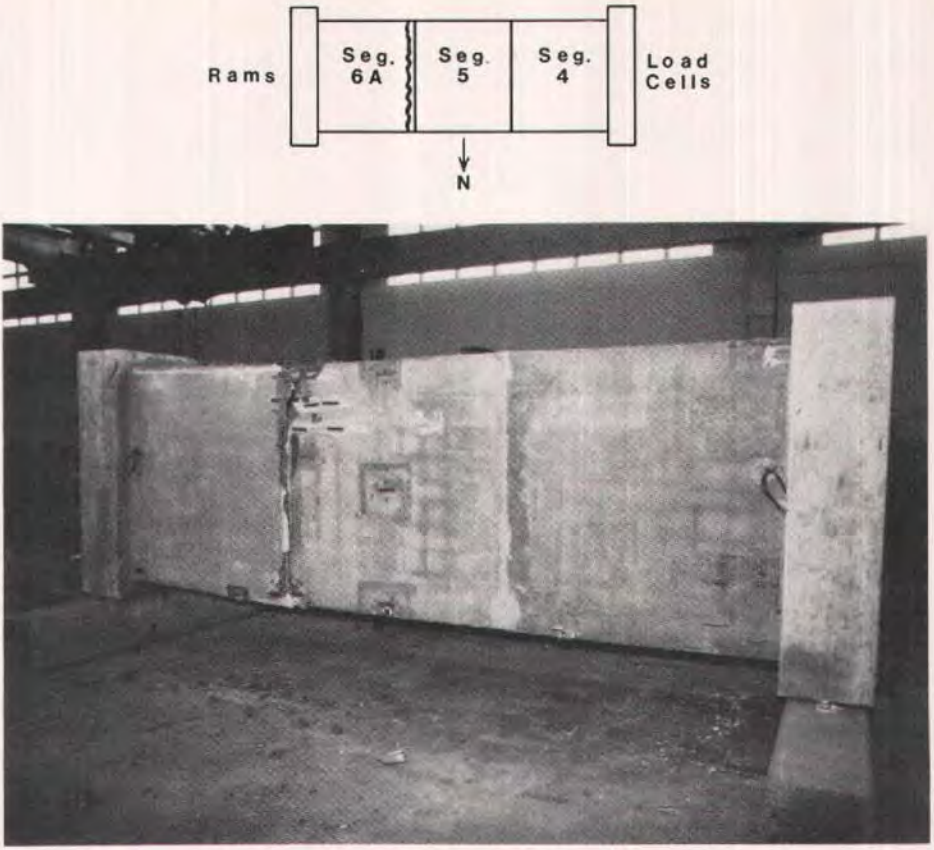

Fig. 31. Specimen 2A — Orientation of specimen and overall view of north plate showing buckling in Segment 6A.

The current AASHTO Specifications control thin plate buckling of steel members by restricting the width of plates through utilization of stiffeners. These restrictions are based on the studies of thin plate buckling characteristics of steel members. Similar design criteria have been developed for thin plates of concrete as a result of this study. The buckling failure mode for thin plates of concrete is brittle compared to the ductile behavior of steel. This brittle type failure indicates that a conservative code provision should be adopted pending further studies of thin plate buckling.

Therefore, it is recommended that plate thinness be limited to:

$$\frac{\text{Width } b}{\text{Thickness } t} \leq 10 \qquad (2)$$

without the rational analysis provided by this study. This limit applies only to rectangular hollow piers with $k = 4.0$. Other limits must be established for differing bridge member configurations. This limit would insure that pier design would be controlled by overall stability rather than local plate buckling.

It was previously stated that the tensile strength and modulus of rupture of high strength concrete follow the trends established for normal strength concrete. This implies that high strength concrete flexural members designed to the normal allowable tension stress cri-

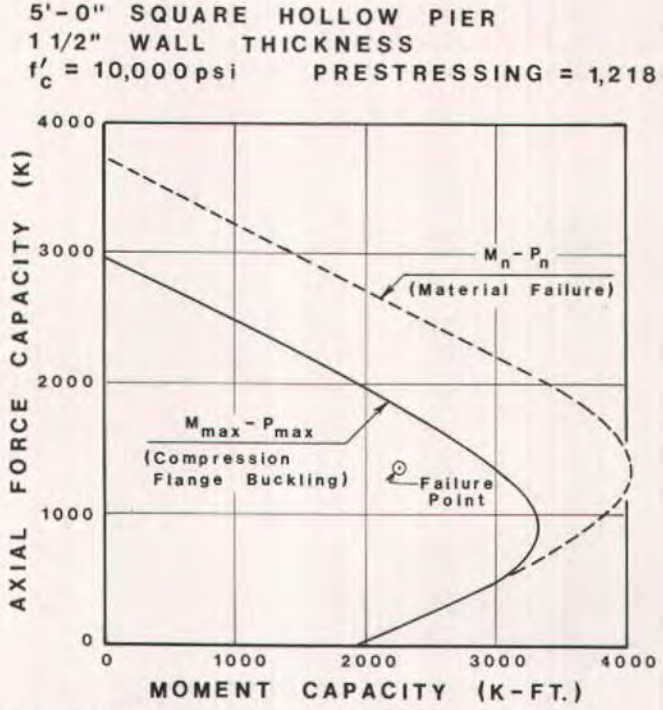

Fig. 32. Specimen 2A — Interaction diagram.

teria will exhibit a superior margin of safety against cracking under service load conditions, because the nominal margin of $1.5\sqrt{f'_c}$ is approximately 40 percent greater for 10,000-psi (70 MPa) concrete than for 5000-psi (35 MPa) concrete. Full advantage could be taken of this fact by revising allowable stress criteria in the following manner:

1.6.6—ALLOWABLE STRESSES

(B) Concrete

(2) Stress at service load after losses have occurred; tension in the precompressed tensile zone

(a) For members with bonded reinforcement:

For normal weight concrete $..7.5\sqrt{f'_c}$ – 106 psi

For sand-lightweight concrete $..6.3\sqrt{f'_c}$ – 106 psi

For all other lightweight concrete $..5.5\sqrt{f'_c}$ – 106 psi

(b) For severe corrosive exposure conditions, such as coastal areas:

For normal weight concrete $..7.5\sqrt{f'_c}$ – 318 psi

For sand-lightweight concrete $..6.3\sqrt{f'_c}$ – 318 psi

For all other lightweight concrete $..5.5\sqrt{f'_c}$ – 318 psi

This proposed code revision would enable the designer to provide a constant margin of safety against flexural cracking in prestressed girders. That is, the same increase of applied moment over design service load moment will cause flexural cracking, irrespective of concrete strength. The allowable stresses given here are calibrated against the AASHTO standard of 5000 psi (35 MPa) (see Article 1.6.6) and the present criteria of $6\sqrt{f'_c}$ and $3\sqrt{f'_c}$ allowable tension allowed for normal and severe exposure, respectively.

SUMMARY

Production and utilization of high strength concrete is rapidly becoming a viable concept in construction. Its application to precast prestressed concrete is readily apparent. The analytical design studies discussed demonstrate the benefits of using high strength concrete in flexural members in addition to compression members. These benefits include increased span lengths, reduced dead loads, and greater load capacities.

The potential for using thin plates of concrete fabricated on flat beds in the customary manner of the precast concrete industry is shown to be advantageous. The analytical studies resulting in the development of a computer program make a rational analysis of these thin plates feasible. This would insure control of the section by design criteria other than local buckling of that thin plate.

The current AASHTO[8] Specifications are not conducive to the use of high strength concrete. Although use is not restricted, Article 1.6.6 does not encourage its use. Further, the restrictions on thickness of member and cover over steel do not permit full utilization of the high stength dense concrete that could be provided for thin sections. These criteria need to be constantly reviewed by code authorities and changes made similar to the provisions presented in this report. Continuing efforts should be made by professional bodies, governmental agencies, and code authorities to more rapidly implement into practice application of the knowledge being developed by numerous researchers on the application of high strength concrete to structural members.

REFERENCES

1. Freedman, S., "High Strength Concrete," *Modern Concrete*, V. 34, Nos. 6-10 , October 1970, pp. 29-36; November 1970, pp. 28-32; December 1970, pp. 21-24; January 1971, pp. 15-22; and February 1971, pp. 16-23.
2. Blick, R. L., "Some Factors Influencing High Strength Concrete," *Modern Concrete*, V. 36, No. 12, April 1973.
3. Chicago Committee on High-Rise Buildings, "High Strength Concrete in Chicago High-Rise Buildings," Report No. 5, February 1977.
4. Nilson, Arthur H., and Slate, Floyd O., "Structural Properties of Very High Strength Concrete," Second Progress Report, NSF Grant ENG 78 05124, School of Civil and Environmental Engineering, Cornell University, Ithaca, New York, 1979.
5. Wang, P. T., Shah, S. P., and Naaman, A. E., "Stress-Strain Curves for Normal and Lightweight Concrete in Compression," *ACI Journal*, V. 75, No. 11, November 1978, pp. 603-611.
6. Kaar, P. H., Hanson, N. W., and Capell, H. T., "Stress-Strain Characteristics of High Strength Concrete," Research and Development Bulletin RD051.01D, Portland Cement Association, Skokie, Illinois, 1977.
7. Perenchio, W. F., and Klieger, P., "Some Physical Properties of High Strength Concrete," Research and Development Bulletin RD056.01T, Portland Cement Association, Skokie, Illinois, 1978.
8. AASHTO, *Standard Specifications for Highway Bridges*, Twelfth Edition, American Association of State Highway and Transportation Officials, Washington, D.C., 1977.
9. ACI Committee 318, "Building Code Requirements for Reinforced Concrete (ACI 318-77)," American Concrete Institute, Detroit, Michigan, 1977.
10. Franklin, D. H., "Shubenacadie Bridge Tames Angry River," *Concrete International*, V. 1, No. 2, February 1979, pp. 73-82.
11. Priest, H. M., *Design Manual for High Strength Steels*, U.S. Steel Company, Davis & Ward, Inc., Pittsburgh, Pennsylvania, 5th Printing, 1957.
12. Bleich, F., *Buckling Strength of Metal Structures*, McGraw-Hill Book Company, 1952.

* * *